Aging and deaging effects in shape memory alloys

Dezhen Xue, Yumei Zhou, Xiangdong Ding, Turab Lookman, Jun Sun, and Xiaobing Ren

Aging and Deaging Effects in Shape Memory Alloys

Dezhen Xue,[1,2] Yumei Zhou,[1] Xiangdong Ding,[1,2,*,†] Turab Lookman,[2,*,‡] Jun Sun,[1] Xiaobing Ren[1,3]

1. *Multi-disciplinary Materials Research Center, Frontier Institute of Science and Technology, State Key Laboratory for Mechanical Behavior of Materials, Xi'an Jiaotong University, Xi'an 710049, China*

2. *Theoretical Division and Center for Nonlinear Studies, Los Alamos National Laboratory, Los Alamos, New Mexico 87545, USA*

3. *Ferroic Physics Group, National Institute for Materials Science, Tsukuba, 305-0047, Ibaraki, Japan*

[*] *Corresponding author.*

[†] *dingxd@mail.xjtu.edu.cn*

[‡] *txl@lanl.gov*

Physical properties in shape memory alloys are known to change as a result of aging over time. However, undesired aging effects in the martensite phase can be eliminated once the aged martensite is brought into the parent phase, often referred to as deaging. We propose a Landau free energy model to study the aging and deaging of martensite. These two effects can be modeled via the increase and decrease of an internal field which adopts the same "symmetry" as the crystal symmetry of the host lattice. Time dependent simulations based on our model successfully reproduce many of the observed martensite aging effects such as martensite stabilization, rubber-like behavior, domain memory effect and aging of the elastic modulus, as well as deaging effects in the parent phase including elimination of martensite aging and parent phase stabilization. Furthermore, we predict the time dependent change of elastic modulus and the stress-strain response in the parent phase, which need to be verified experimentally.

I.   INTRODUCTION

Shape memory alloys (SMAs) undergo a martensitic transformation between the high symmetry parent phase and the low symmetry martensite phase. This leads to the shape memory effect (SME) and superelasticity (SE), which have numerous applications in devices such as actuators and sensors. [1] However, a number of SMAs (including Au-Cd, Au-Cu-Zn, Cu-Zn-Al, Cu-Al-Ni, Ti-Ni-Hf and Ni-Mn-Ga) exhibit aging effects in the martensite phase in which there is a gradual change of physical properties with aging time. [2-7] These martensite aging effects, which dramatically influence the reliability of SMA devices, are undesirable in applications in general. Usually the simplest way to eliminate such aging effects in SMAs is to make the aged martensite experience a reverse transformation to the parent phase. The process is referred to as deaging and it is closely related to the martensite aging process. [3, 8-10] Therefore, these effects have attracted considerable attention, not only in probing their time dependent characteristics, but also in understanding their physical origin.

The martensite aging effects have been actively studied over the past decades and usually involve the following four aspects. [11-13] (1) The rubber-like behavior (RLB), that is, the martensitic alloy after being aged for some time in the martensite phase exhibits *recoverable* or pseudo-elastic deformation behavior. [4] (2) The martensite stabilization effect, i.e. the martensite phase becomes more stable after aging, which is due to the fact that the reverse martensitic transformation temperature *increases* with increasing aging time. [14, 15] (3) Aging effects on the "small signal" dynamic properties, i.e., the gradual increase of elastic modulus and decrease of internal friction with aging time. [16, 17] (4) Aging induced domain memory effects in the martensite phase, i.e., the same twin-variant pattern of an aged martensite can be restored after a loading-unloading cycle; similar domain recovery can occur if aged martensite is heated into the parent phase and subsequently cooled back to the martensite. [10, 13]

The conjugate phenomenon to martensite aging is the deaging effect which refers to the *disappearance* of martensite aging effects, once the aged martensite experiences a reverse transformation into the parent phase. [3, 8, 9] This is accompanied

by the disapperance of the RLB after holding the system in the parent phase for some time. [3, 8] However, the time dependent characteristics of such deaging effects have not been well studied as the martensite aging effects but usually involve the following two aspects: (1) The parent phase stabilization, which refers to the gradual decrease of the martensitic transformation temperature with holding time in the parent phase, [9] and (2) The existence of a residual domain contrast, that is, on heating the aged martensite above A_f (the finishing temperature for reverse martensitic transformation) so that it transforms into the cubic parent phase, a martensite-like "residual contrast" remains in the parent phase and gradually disappears with increasing holding time in the parent phase. [10]

Many studies have examined the origin of the martensite aging phenomena and several models have been proposed (see Refs. 11, 12 for a detailed review of these models of aging). Among them, the symmetry conforming short range order (SC-SRO) principle appears to explain available experimental observations qualitatively and is indirectly corroborated by TEM observations and small changes in the symmetry of the XRD profile. [4, 10, 13] The main idea of the SC-SRO principle is that the local distribution of point defects tends to follow the crystal symmetry when in equilibrium.[4] During martensite aging, the local distribution of point defects with parent symmetry (high) gradually conforms to the crystal symmetry of the martensite phase by reconfiguration of vacancies/anti-site defects. [4] However, these models largely ignore the deaging effects. Recently, Deng et al. probed the change of short-range order parameters during deaging by combining Monte Carlo and molecular dynamics simulations and showed that the SC-SRO principle can be valid for deaging as well.[18, 19]

Based on the idea of the SC-SRO principle, Ohta and co-workers developed a Landau-type model to describe the martensite aging phenomena by considering a secondary slow variable associated with martensite aging. [20, 21] They successfully reproduced two aspects of the martensite aging, that is, the RLB and the martensite stabilization, but not the increase of the elastic modulus or the restoration of domain memory effects. Very recently, K. Anna and co-workers considered the secondary slow variable to be an internal stress field with very long relaxation time associated with the SC-SRO tendency of point defects. [22-24] This also reproduced the martensite stabilization effects. [22, 23] As these studies are all based on a 1D homogenous Landau

model, investigations on domains (twin structure), which are at the heart of martensite behavior in SMAs, were not undertaken. In addition, the deaging effects in the parent phase were not studied. Therefore, despite the above progress, two important problems remain to be addressed. These are the theoretical description of the two aspects of martensite aging, namely, the domain memory effect and aging of elastic modulus, and deaging effects. Since aging and deaging are closely related, we will consider how they may be described within the same theoretical description.

We will model martensite aging through the increase of an internal stress field within each martensite variant, consistent with the SC-SRO principle. Similarly, deaging is considered as the decrease of the prior martensite aging produced internal stress field, which adopts the same "symmetry" as the parent phase. We will show that time dependent Ginzburg-Landau (TDGL) simulations can successfully reproduce the experimentally observed four aspects of martensite aging effects discussed above, as well as the corresponding deaging effects. Furthermore, we also predict the time dependent change of elastic modulus and the stress-strain response in the parent phase. Our paper is organized as follows. In Section II, we discuss the mesoscale model that captures the salient aspects of a martensitic transformation as well as the evolution of point defects via an internal stress field. Sections III and IV describe the results from our model for aging in the martensite as well as deaging in the parent phase. Here we describe in detail the effects on rubber-like behavior, stabilization, domain patterns and aging of the elastic modulus. We compare our results to experimental measurements and finally we provide an overview of the range of aging/deaging phenomena that our model can describe.

II.   FORMULATION OF THE GINZBURG-LANDAU MODEL

A.   Internal stress field associated with martensite aging and deaging

As introduced previously, martensite aging is generally attributed to the rearrangement of point defects within crystal lattices.[4, 19] Deaging in the parent phase is closely related to prior martensite aging and recent studies have shown that deaging process is also accompanied with a redistribution of point defects.[9] Since the reconfiguration of point defects is always accompanied by a local straining/stressing of the crystal lattice[22-25], we consider the reconfiguration process of point defects as equivalent to the evolution of an internal stress field ρ. If the SC-SRO principle is

valid, the point defects reconfigure themselves slowly following the symmetry of the crystal lattice. [4, 10] Accordingly, the internal stress field ρ , adopts the same "symmetry" as the crystal lattice. This requires: (1) in the martensite phase, ρ should be non-zero corresponding to the non-cubic symmetry of martensite; (2) within each variant of a twin, ρ should have a different value as the orientations of martensite variants are different; (3) in the parent phase, ρ should be zero corresponding to the cubic symmetry of the parent phase; and (4) the evolution of ρ should be much slower than the martensitic transformation, as the former requires diffusion of point defects and the latter requires only a small amount of shearing of atoms.

To this end, the requirements can be fulfilled by letting the internal field ρ assume a functional form that represents a free energy potential with two wells for the minima. The influence of ρ on the system is given by the coupling of ρ and the transformation strain. Figure 1 schematically shows the effects of ρ on the local Landau free energy potential. The typical multi-variant martensite is schematically shown in Fig. 1(a1) and the corresponding Landau free energy curves of different variants are shown in Figs. 1(a2) and 1(a3) which include the influence of ρ (i.e. $\rho \neq \mathbf{0}$). For comparison, the normal Landau free energy without the influence of ρ (i.e. $\rho = \mathbf{0}$) is shown by the dotted line in these figures. As readily seen from Figs. 1(a2) and 1(a3), the introduction of ρ results in a local symmetry-breaking of the Landau free energy curves, which will give preference to certain domain states. Note that this local symmetry-breaking effect for ρ persists even in the parent phase, as shown in Figs. 1(b2) and 1(b3) ($\rho \neq \mathbf{0}$). The dotted lines in Fig. 1(b1) denote the original areas occupied by martensite variants and the Landau free energy curves with $\rho = \mathbf{0}$ are shown in Figs. 1(b2) and 1(b3) by the dotted lines. We will show later that such a Landau description captures much of the observed martensite aging and deaging effects.
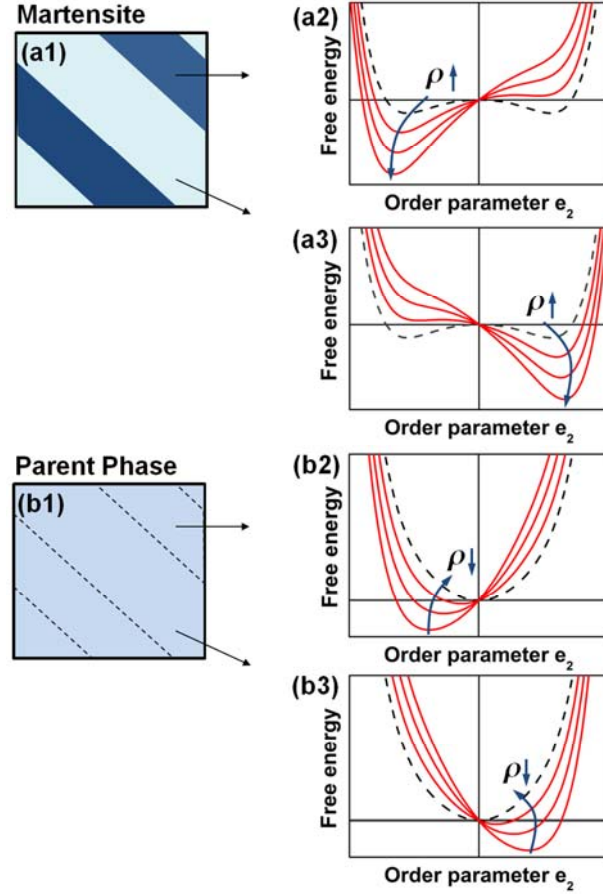
Fig.1. A schematic illustration of the local Landau potential after martensite aging, showing the influence of a defect field, ρ. (a1) The typical martensite domain pattern of twin variants with strain order parameter $e_2 = \dfrac{1}{\sqrt{2}}(\varepsilon_{xx} - \varepsilon_{yy})$; (a2) and (a3) show the Landau potential in the two variants with $\rho \neq 0$ and $\rho = 0$ (dotted line). The curved arrows in (a2) and (a3) indicate the change of local Landau potential with increasing ρ (vertical arrow). (b1) The dotted lines denote the signature of the original domain walls for the martensite variants. (b2) and (b3) show the Landau potential in parent phase with $\rho \neq 0$ and $\rho = 0$ (dotted line). The curved arrows in (b2) and (b3) indicate the change of local Landau potential with decreasing ρ (vertical arrow).

B.   Formulation of free energy

We consider a 2D version of the cubic to tetragonal transformation appropriate for materials such as FePd or InTl. Our ideas are quite general and apply to any transformation; however, the square to rectangular martensitic transformation illustrates the key aspects of martensite aging and deaging effects without sacrificing simplicity. The symmetry adapted strains e_1, e_2 and e_3 represent hydrostatic,

deviatoric and shear modes, respectively, [26-28] where $e_2 = \frac{1}{\sqrt{2}}(\varepsilon_{xx} - \varepsilon_{yy})$ is the order

parameter (OP) responsible for the transition, and $e_1 = \frac{1}{\sqrt{2}}(\varepsilon_{xx} + \varepsilon_{yy})$ and $e_3 = \varepsilon_{xy}$

are the non-OP strains. The $\{\varepsilon_{ij}\}$ are the linearized strain components defined

by $\varepsilon_{ij} = \frac{1}{2}(\frac{\partial u_i}{\partial x_j} + \frac{\partial u_j}{\partial x_i})$, where u_i is the displacement component. Incorporating the

influence of the internal stress filed ρ associated with martensite aging, the total free-

energy density is written as the summation of five contributions:

$$G = \int d\mathbf{r}[f_h(e_2) + f_{grad}(\overline{\nabla}e_2) + f_{non-OP}(e_1, e_3) + f_{aging}(\rho, e_2) + f_{load}(\sigma_{11}, e_2, e_2)]. \qquad (1)$$

The first is the homogeneous Landau part accounting for the required non-linearities

in the OP for the transition. The f_{grad} is the Ginzburg (gradient) term in the OP for the

interface energy cost. The f_{non-OP} is the contribution due to the non-OP components of

the strains that we assume to be harmonic and it will give rise to a long-range

repulsive force. The f_{aging} is the contribution associated with martensite aging, which

we assume to be a double well potential. Here the field ρ is symmetry sensitive by

virtue of its coupling to the symmetry related order parameter (OP) strain. The f_{load} is

the external stress field component (uniaxial tension). Thus, the form of the free

energy contributions is chosen to be (Ref 28):

$$f_h(e_2) = \tfrac{1}{2} A_2(T - T_C)e_2^2 + \tfrac{1}{4}\beta e_2^4 + \tfrac{1}{6}\gamma e_2^6, \qquad (2)$$

$$f_{non-OP}(e_1, e_3) = \tfrac{1}{2} A_1 e_1^2 + \tfrac{1}{2} A_3 e_3^2, \qquad (3)$$

$$f_{grad}(\overline{\nabla}e_2) = \tfrac{1}{2}\kappa |\overline{\nabla}e_2|^2, \qquad (4)$$

$$f_{aging}(\rho, e_2) = \tfrac{1}{2}\varphi(T - T_C)\rho^2 + \tfrac{1}{4}\psi\rho^4 - \mu e_2\rho, \qquad (5)$$

$$f_{load}(\sigma_{11}, e_1, e_2) = -\sigma_{11}\varepsilon_{11} = -\tfrac{\sqrt{2}}{2}(e_1 + e_2)\sigma_{11}. \qquad (6)$$

where the coefficients A_1, A_2, A_3 are second order elastic constants with A_2 linearly

dependent on temperature and describing the softening in the deviatoric shear strain

(e_2), β, γ are higher order elastic constants that can be determined from

thermodynamic, lattice parameter data and the nature of the first order transition, κ is

7

the cost of creating inhomogeneities or gradients in the elastic strain, ϕ, ψ and μ are coefficients that control the aging process, and σ_{11} is the applied uniaxial stress. ϕ, ψ control the magnitude of the internal field ρ and μ is the coefficient of the coupling term, which determines the interaction between the internal field ρ and order parameter e_2.

The three strain components e_1, e_2, e_3 are not independent because they are the derivatives of the same underlying displacement field. Therefore, they must satisfy compatibility constraints in order to ensure lattice integrity. Formally, the constraint is expressed through the Saint-Venant equation in 2D, $\nabla^2 e_1(r) - \sqrt{8} \nabla_x \nabla_y e_3(r) = (\nabla_x^2 - \nabla_y^2) e_2(r)$.[27] After minimization of the total free energy with respect to e_1 and e_3 by taking into account the elastic compatibility condition, we obtain $f_{non-OP} = \int e_2(\vec{r}) U_1(\vec{r} - \vec{r}') e_2(\vec{r}') d\vec{r}'$ and $f_{load} = -\frac{\sqrt{2}}{2} e_2 \sigma_{11} + \frac{\sqrt{2}}{2} \int [e_2(\vec{r}) U_3(\vec{r} - \vec{r}') \sigma_{11}(\vec{r}') - \frac{1}{2} \sigma_{11}(\vec{r}) U_2(\vec{r} - \vec{r}') \sigma_{11}(\vec{r}')] d\vec{r}'$. The $U_1(\vec{r} - \vec{r}')$, $U_2(\vec{r} - \vec{r}')$ and $U_3(\vec{r} - \vec{r}')$ are anisotropic kernels and provide the long range interaction between strained regions. These kernels can be more simply expressed in Fourier space:

$$U_1(\vec{k}) = \frac{(k_x^2 - k_y^2)^2}{\vec{k}^4 / A_1 + 8 k_x^2 k_y^2 / A_3}, \qquad (7)$$

$$U_2(\vec{k}) = \frac{8 k_x^2 k_y^2 / (A_1 A_3)}{\vec{k}^4 / A_1 + 8 k_x^2 k_y^2 / A_3}, \qquad (8)$$

$$U_3(\vec{k}) = \frac{\vec{k}^2 (k_x^2 - k_y^2) / A_1}{\vec{k}^4 / A_1 + 8 k_x^2 k_y^2 / A_3}. \qquad (9)$$

The kinetics of the transformation is given by,

$$\frac{\partial e_2}{\partial t} = -\frac{\delta G}{\delta e_2}, \qquad (10)$$

and the evolution of the internal stress field ρ is described through the equation:

$$\tau(T) \frac{\partial \rho}{\partial t} = -\frac{\delta G}{\delta \rho} = -- \frac{\delta (f_h + f_{grad} + f_{non-OP} + f_{aging} + f_{load})}{\delta \rho}, \qquad (11)$$

8

where G is the total free energy and $\tau(T)$ is the relaxation time. It has been shown that the aging effect in both martensite and parent phases follows the standard Arrhenius relation for the diffusion process; thus $\tau(T)$ reads

$$\tau(T) = \tau_0 \exp(-Q/T) \qquad (12),$$

where Q is the activation energy for the aging process, and τ_0 is a prefactor related to attempt frequency and the intrinsic nature of the lattice[18].

The continuum model has been implemented numerically on a two-dimensional 128×128 lattice with periodic boundaries to investigate the martensite aging and deaging effects. The equations are solved numerically using a finite difference scheme with a fast Fourier transform facilitating the handling of the long range kernel for the elastic interaction. We found an Euler level scheme to be adequate with discretization $\delta x = 1$, $\delta y = 1$ and $\delta t = 0.02$. Since a number of SMAs show martensite aging and deaging effects and we are interested in a qualitative understanding of the physical mechanisms, we chose reduced values of the parameters: A_1=1.0, A_2=2.27, A_3=4.54, β=-276, γ=4.86×10^5, κ=1.0, T_C=1.0, φ=1.0, ψ=5520 and μ=2.5. The chosen parameters are appropriate for FePd, [29] and the last three coefficients in Eq.(5) were chosen so that the minima of the ρ field were comparable to those for the strain, e_2. The coefficients in Eq. (12) were fixed during our calculation with Q=0.2 and τ_0 =5000. The initial system, made of 100% parent phase, includes random fluctuations around $e_2 = 0$. It is instantaneously quenched to a temperature well below the transformation temperature and held at this temperature for martensite aging. The well aged martensite state is instantaneously heat-quenched to a temperature well above the transformation temperature and held at this temperature for deaging. The heating and cooling process for determination of transformation temperature was carried out in temperature steps of 0.05 and the system was allowed to relax for 1000 simulation steps during the course of each temperature step.

III.   MARTENSITE AGING EFFECTS

In this section, the above time-dependent Ginzburg-Landau model is employed to study the four aspects of martensite aging discussed: (1) rubber like behavior; (2) martensite stabilization; (3) domain memory effects and (4) Aging of the elastic

9

modulus. The system was quenched from the high temperature parent phase to the low temperature martensite phase and then held at a constant temperature for a certain time. The time is long enough (4×10^5 simulation steps) for the internal stress field ρ to be saturated, corresponding to the point defect redistribution process.

A.   Rubber-like behavior (RLB)

We first study the deformation behavior of simulated SMA as a function of aging time and aging temperature. An example in which the system is aged at T=0.3 for different aging times is shown in Fig. 2(a). The unaged martensite shows pseudo-plastic deformation behavior (t=1.0×10^4 curve in Fig. 2(a)), as a result of an irreversible twinning process in the martensite phase. With increasing aging time, the deformation behavior changes to pseudoelastic or RLB, as the t=1.0×10^5 curve and curves for longer times in Fig. 2(a) show. Such evolution is qualitatively the same at different temperatures in the martensite phase. It has been known experimentally that a large number of martensitic alloys such as Au-Cd,[3, 14, 17] Au-Cu-Zn,[5] Cu-Zn-Al,[30] Cu-Al-Ni,[31] In-Tl,[32] and Ti-Pd[15] exhibit this unusual evolution of deformation behavior from pseudo-plastic to RLB with aging in the martensitic phase. Accompanying the evolution of deformation behavior is the gradual increase of critical stress for de-twinning (rearrangement of martensite variants). The aging time dependence of the critical stress is shown in Fig.2(b). We note that the critical stress shows similar tendency with aging time at different aging temperatures. The change is greater at higher aging temperatures where the stress saturates at shorter aging time due to the temperature dependence of the relaxation time $\tau(T)$. The same behavior is also observed in experiments on the trigonal (ζ_2') martensite phase of a furnace-cooled Au-49.5at.%Cd alloy, i.e. the critical stress for rearrangement of the martensite variants increases with aging time and finally saturates.[3, 13]

The appearance of RLB with aging time can be as ascribed to the growth of the internal stress field ρ. Since the evolution of ρ is rather slow, at the early stage of aging (t=1.0×10^4 simulation steps), the internal stress field ρ remains quite small and has little effect on the deformation behavior. Thus, the normal pseudo-plastic deformation behavior is observed in the simulations. With increase of aging time, the internal stress field ρ gradually increases within each martensite variant. The

10

field ρ will favor certain variant orientations (the tilted free energy curve shown in Figs. 1(a2) and 1(a3)). As a result, the martensite will adopt the same twinning pattern after unloading and the strain is thus reversible. The corresponding microstructure domain memory effect will be shown in section III.C. Note that the RLB intrinsically differs from superelasticity, which occurs by means of stress-induced martensitic transformation from the high-temperature parent phase on loading and its subsequent reverse transformation on unloading. Furthermore, in the presence of ρ, each martensite variant was stabilized along its original orientation, which makes the rearrangement of variants more difficult. This results in the increase of critical stress.

B.   Martensite stabilization effect

Here we show results for the martensite stabilization effect, i.e. an increase of the reverse martensitic transformation temperature with aging time. To examine the influence of the internal stress field, ρ, we study the aging temperature and aging time dependence of the reverse martensitic transformation temperature. The transformation temperature was determined by the minimum in the elastic modulus vs.

temperature curve, as shown in inset of Fig. 3(a).[33] The elastic modulus was calculated by taking the second derivative of the total free energy, that is,

$$E(T,t) = A_2(T - T_C) + 3\beta e_2^2 + 5\gamma e_2^4 + 2U_1(\bar{r}). \qquad (13)$$

Fig. 3(a) shows the results for a system aged at T=0.3 for different aging time. The temperature corresponding to the minimum in the elastic modulus gradually increases as the aging time increases. Fig. 3(b) shows the time dependence of the reverse martensitic transformation temperature at different aging temperatures. Such time dependent behavior has been experimentally observed in several martensitic alloys including Au-Cd,[3, 14] Cu-Zn-Al,[8, 34] and Ni-Ti-Hf[6]. Similar to the change of critical stress in Fig.2(b), the reverse transformation exhibits an increase with aging time for different aging temperatures, but the higher aging temperature results in greater change. Furthermore, it should be noted that the higher aging temperature also gives rise to a larger change in the saturated value of the reverse transition temperature, which agrees with aging experiments on the physically similar ferroelectric materials.[35] As shown by the tilted free energy curves in Figs. 1(a2) and 1(a3), an increase of internal stress field ρ leads to deeper energy minima. This means that the martensite phase will exist in a wider temperature range, thus explaining the martensite stabilization effect.
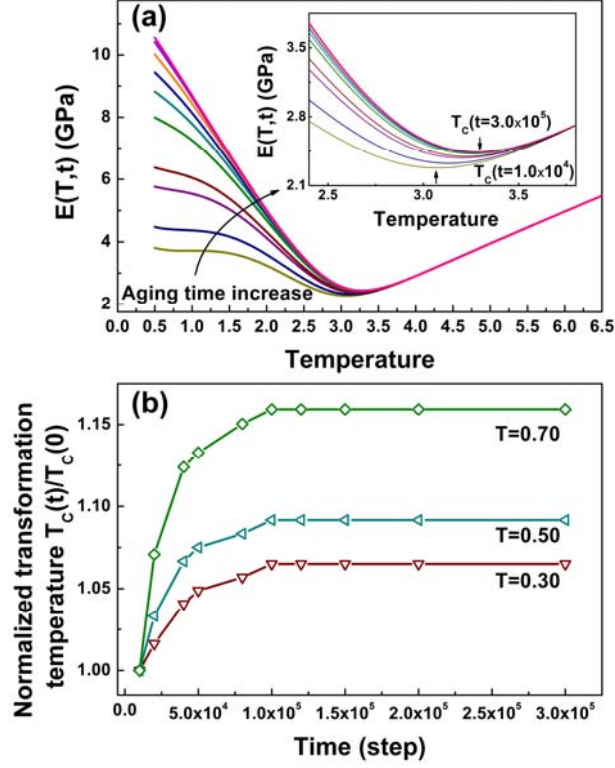
12

C.   Domain memory effects

As mentioned in section III.A, martensite aging can give rise to a reversible twinning process, and this will result in the reappearance of identical twin patterns. This is referred to as the domain memory effect. Such an aging induced domain memory effect not only occurs during the loading and unloading cyclic process, but also during the heating and cooling cycles. The former is responsible for the RLB in SMAs [4], and the latter can give rise to the so-called "aging-induced two way shape memory effect" [10].

We first study the domain memory effect during a loading and an unloading cycle. Fig. 4(a) shows normal pseudo-plastic deformation behavior at the early stage of aging (t=1.0×10^4 simulation steps). During loading, the characteristic martensite multi domain/variant pattern becomes single variant along the stress direction. As the internal stress field ρ is far from being well developed at this early stage, different domains (twins) actually have the same energy. Therefore, at the mesoscopic level,

13

the multi martensite domain pattern cannot be reproduced after unloading and the single variant is retained, as shown in the microstructures in Fig.4(a). With increasing aging time, the situation gradually becomes different because the internal stress field ρ within each variant increases and makes such a domain state favored (with lower energy as shown in Fig.1(a2) or Fig.1(a3)). An example after aging for $t=5.0\times10^5$ simulation steps is shown in Fig.4(b). When aged martensite is deformed, domain reversal (i.e., detwinning) occurs as a result of strain accommodation. Since such de-twinning process is diffusionless, the internal stress field ρ will not change and is inherited in the new domain. As a result, the internal stress field ρ will have different orientations in such a configuration, so the new domain state is not stable. Therefore, a driving force that tries to restore the original domain is engendered. As a result, during unloading, this restoring force reverts the new domain to the original one, and macroscopically the sample exhibits pseudoelastic behavior (Fig. 4(b)). The comparison of unaged and aged martensite on domain pattern evolution has been performed experimentally in a typical martensitic alloy Au-Cd[13] and our model well reproduces the experimental observations.
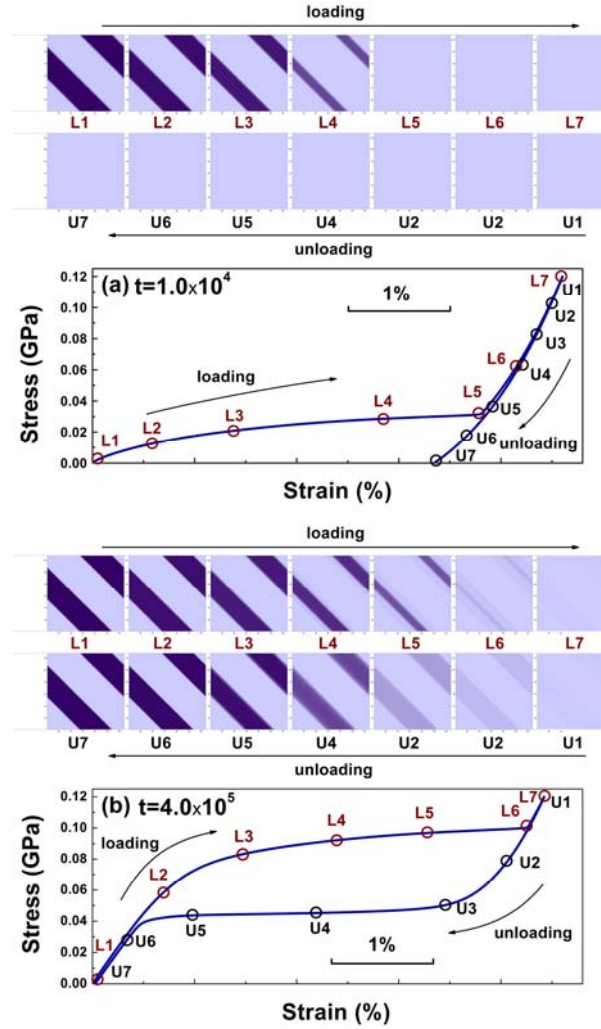
Fig.4. The domain evolution during loading and unloading for T=0.3. (a) For unaged martensite which shows normal plastic deformation, the initial multi-domain state (L1) gradually becomes a single-domain state (L7) upon loading and this single-domain state (U1) is retained after unloading (U7). The domain pattern cannot be memorized. (b) For aged martensite which shows psudoelastic deformation (RLB), the initial multi-domain state (L1) gradually becomes single-domain state (L7) upon loading and this single-domain state (U1) gradually recovers to the identical multi-domain state (U7) upon unloading. The same domain pattern (L1 and U7) is restored.

The other domain memory effect occurs during the heating and cooling transformation cycle. The normal transformation cycle is shown in Fig. 5(a). The typical domain pattern (Fig.5 (a1)) was heated to the parent phase (Fig.5 (a2)), followed by quenching to martensite (Fig.5 (a1)). A totally different domain configuration was obtained, since different domain orientations are energetically equivalent. The corresponding experimental results have been seen in a Au-Cd alloy.[13] However, after martensite aging, the internal stress field ρ in different

15

martensite domains orient differently, following their corresponding crystallographic orientation (the orientation given by e_2 here). When the aged martensite (Fig. 5(b1)) transforms into the cubic parent phase (Fig. 5(b2)) by reverse transformation, the OP e_2 that relates to crystal symmetry becomes zero. However, due to the long relaxation time, the internal stress field ρ within each of the martensite domains is inherited by the cubic parent phase. Consequently, there exists a different orientation of internal stress field ρ in the parent phase between regions that previously were martensite domains. This orientation difference in the internal stress field ρ will produce a "domain like contrast" pattern in the cubic parent phase (Fig. 5(b2)) that is identical to the martensite domain pattern shown in Fig. 5(b1). Such domain contrast has been observed experimentally by in-situ TEM.[10] Now, when we let this "nonequilibrium" parent phase (Fig. 5(b2)) transform by cooling into martensite again, it is apparent that it will adopt the previous martensite domain pattern (Fig. 5(b3)) so as to make the internal stress field ρ conform to the martensite crystallographic orientation everywhere, as a consequence of coupling between e_2 and ρ. Such "domain-pattern memory" induced by martensite aging has also been found experimentally in a Au-Cd martensitic alloy[13] and $(Ba,Sr)TiO_3$ ferroelectric single crystal[36] by optical microscopy. The macroscopic manifestation of this mesoscopic memory is the memory of the shape of previous martensitic alloy, i.e. two-way shape memory effect[10].
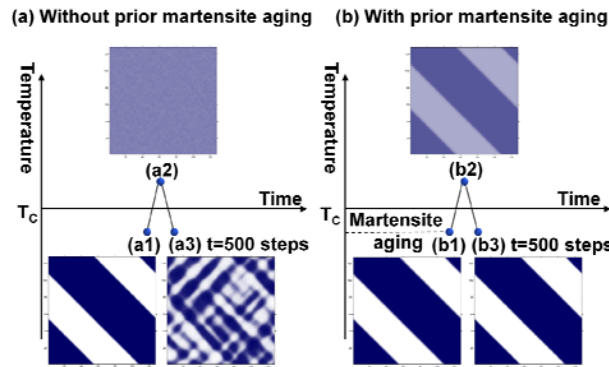

Fig.5. The domain evolution during temperature induced martensitic transformation. For unaged martensite, a typical domain pattern (a1) was heated to the parent phase (a2), followed by a quench to martensite (a3). The domain pattern cannot be memorized. For aged martensite, a typical domain pattern (b1) was heated to the parent phase (b2) followed by a quench to martensite (b3). The same domain pattern as (b1) is restored.

D. Aging of elastic modulus

Fig. 6 shows the evolution of elastic modulus with aging time at different aging temperatures. The elastic modulus is calculated via. Eq.(13). It is clear that the martensite aging effects are qualitatively similar at different aging temperatures, i.e. the elastic modulus gradually increases with increasing aging time and approaches saturation. Two features are noted: the aging rate increases at higher temperatures and the relative change of elastic modulus increases with increasing aging temperature. Such time dependence of the elastic modulus, as well as the mentioned two features are observed experimentally in the furnace-cooled Au-49.5at.%Cd, furnace-cooled Au-50.0at.%Cd and quenched Au-50.0at.%Cd alloys [16], so our model can capture the elastic modulus aging aspect. As shown in Figs. 1(a2) and 1(a3), the growth of the internal stress field ρ not only makes the free energy minimum deeper but also makes it steeper due to the increase of curvature, which is the reason for the elastic modulus increase.
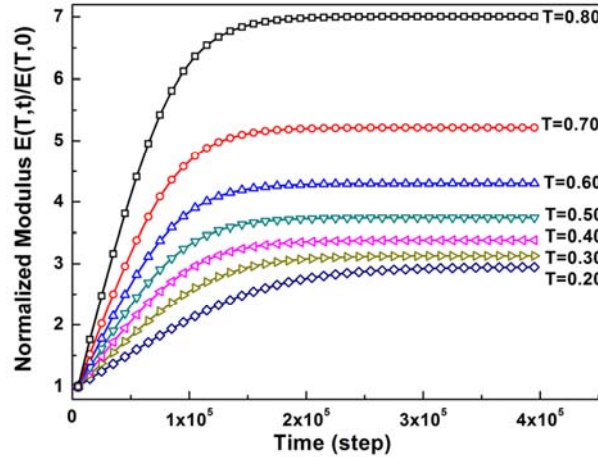

Fig.6. Elastic modulus as a function of aging time at different temperatures showing that increase of temperature stiffens the system and aging at a given temperature leads to rubber-like behavior (RLB). The elastic moduli are normalized by the initial values through $E(T,t)/E(T,0)$.

IV. DEAGING EFFECTS IN THE PARENT PHASE

In this section we show how the time-dependent Ginzburg-Landau model can be used to study deaging effects in the parent phase. In the introduction, we discussed two aspects of deaging. However, as deaging is the conjugate phenomena to

17

martensite aging, we can similarly examine four aspects of deaging: (1) elimination of martensite aging; (2) parent phase stabilization; (3) residual domain contrast and (4) change of stress-strain curve and elastic modulus with aging time. The system was heat-quenched to the parent phase after adequate martensite aging for a relatively long time $(t=1.5\times10^5$ simulation steps) at a constant temperature (T=0.3). The time for deaging in the parent phase is long enough for the internal stress field ρ to vanish.

A.   Elimination of martensite aging

It is well known that deaging will eliminate the martensite aging effects. Deaging refers to the refreshment of martensite, once the aged martensite experiences a reverse transformation into the parent phase. The most pronounced aspect is disappearance of the RLB. We thus first show the elimination of martensite aging from this aspect. After martensite aging (at T=0.3 for $t=5.0\times10^5$ simulation steps), the system exhibits RLB, as shown in Fig. 7(a). When the system was suddenly heated above the reverse transformation temperature, the stress-strain response changes to a linear response (Fig. 7(b)), characterizing the parent phase. Annealing at T= 3.5 in the parent phase for a short time ($t=1.0\times10^4$ simulation steps), the system was quenched again to the martensite phase. As shown in Fig. 7(c), the RLB behavior can still be observed. This indicates that a mere diffusionless transformation into the parent phase is not enough for eliminating the martensite aging effect. Note that the critical stress in Fig. 7(c) becomes smaller compared to the aged martensite in Fig. 7(a), which is caused by the short holding time in parent phase ($t=1.0\times10^4$ simulation steps). If the system is held in the parent phase for a longer period (at T=3.5 for 1.0×10^6 simulation steps), it then exhibits linear deformation behavior (Fig. 7(d)). After quenching back to the martensite phase, the system undergoes a normal plastic-deformation behavior but not RLB, as shown in Fig. 7(e). Thus, the previous martensite aging effect has been removed completely.

After martensite aging, the internal stress field ρ is well established. When such an aged martensite transforms into the cubic parent phase, the OP e_2, becomes zero but the internal stress field remains unchanged. The vanishing of ρ in the cubic parent phase requires an adequate period of time to complete, because it involves rearrangement of point defects. Thus, the elimination of the martensite aging effect

18

involves both the reverse transformation to the parent phase as well as sufficient aging in the parent phase during which the diffusion of point defects can occur.
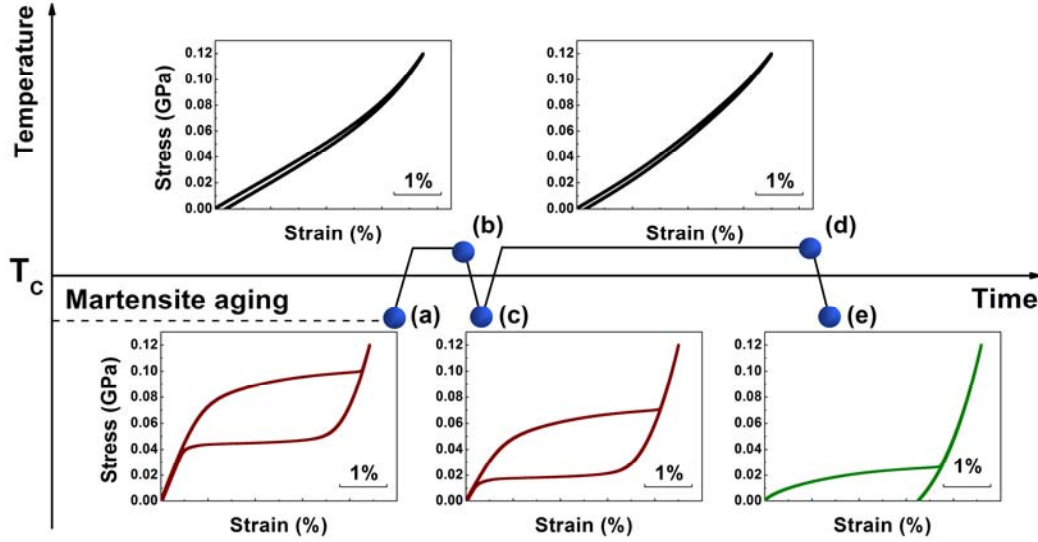

Fig.7. Evolution of the deformation behavior during a heating and cooling cycle for aged martensite. (a) pseudoelastic, rubber-like behavior (RLB) of the aged martensite. The sample was heated up to (b) the parent phase and cooled down to (c) the martensite phase with RLB. The sample was then heated up again to (d) the parent phase and held for 1.0×10^6 simulation steps, followed by cooling down to (e) where the refreshed martensite exhibits normal plastic behavior.

B. Parent phase stabilization effect

Another experimentally observed phenomenon associated with deaging is the decrease of the martensitic transformation temperature with deaging time.[8, 9] This is parent phase stabilization, conjugate to the martensite stabilization effect. It should be noted that parent phase stabilization takes place only when the martensite phase is priorly aged.[9, 18] The transformation temperature was determined by the elastic modulus minima using the elastic modulus vs. temperature curve, as shown in the inset of Fig. 8 and the elastic modulus was calculated following Eq. (13). Fig. 8 shows an example of a sample deaged at T=3.5 for different time periods. The temperature corresponding to the minimum in the modulus gradually decreases with increasing deaging time. Such behavior can be understood as follows. During deaging in the parent phase, the internal stress field ρ gradually vanishes. Since the existence of the internal stress field ρ will promote the martensitic transformation, this effect will

19

gradually disappear with decreasing internal stress field ρ. It should be noted that the decrease of martensitic transformation temperature corresponds to the elimination of the martensite stabilization effect that has been discussed in Section III.B. This also indicates that elimination of martensite aging involves both the reverse transformation and sufficient deaging in the parent phase.
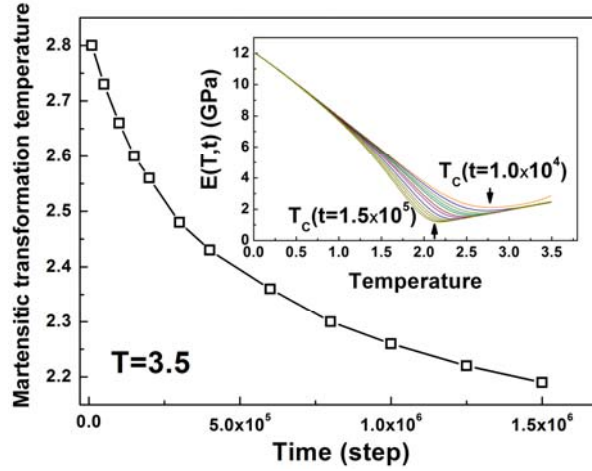
C.   Residual domain contrast

Here we show an interesting observation in the parent phase with prior martensite aging.[10] The well aged martensite phase shows a multi-variant domain pattern in Fig.9(a). After heating to the parent phase, a "domain-like" contrast is observed in Fig. 9(b1) (and also shown in Fig.5(b2)), which is referred as a residual domain contrast [10]. With increasing deaging time in the parent phase (Figs. 9(b1) to 9(b4)), the contrast gradually becomes weaker. After sufficient aging in the parent phase, it totally disappears (Fig.9(b4)). Experimentally, such "residual domain contrast" has been observed in an aged martensitic Au-Cd alloy by in-situ TEM during heating and holding. [10] After quenching this non-contrast parent phase to martensite, a totally different domain pattern from the initial one in Fig. 9(a) is observed in Fig. 9(c). As shown in Figs. 5(b1) and 5(b3), there is domain memory during the heating and cooling cycle. Figs. 9(b1) to 9(b4) indicates that holding the sample in the parent phase for sufficient time will eliminate this domain memory effect. Although after a

20

reverse martensitic transformation, the OP e_2 tends to become zero everywhere, the internal stress field ρ persists e_2 to slightly deviate from zero, in the prior regions of martensite variants. This deviation in different regions will give rise to the residual domain contrast. Following the vanishing of the internal stress field ρ with deaging time, e_2 becomes into zero and consequently the domain contrast gradually disappears.
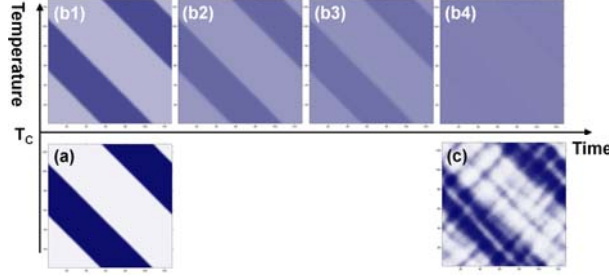

Fig.9. Domain evolution during a heating and cooling cycle and deaging with time in the parent phase. A typical domain pattern of aged martensite (a) was heated up to the parent phase (b1) where residual domain contrast remains. With deaging in the parent phase, such domain contrast gradually disappears (b1 to b4). After quenching to martensite again, a new domain pattern (c) is observed.

D. Change of stress-strain curve and elastic modulus with aging time in the parent phase

We have discussed previously the experimentally observed martensite aging and deaging phenomena. Based on our model, we can also predict the following time dependent change of properties in the parent phase of SMAs. The inherited internal stress field ρ from aged martensite will influence the elastic modulus of the system, similar to that during the martensite aging process. As shown in Fig. 10(a), the calculated elastic modulus of the parent phase from Eq.(13) decreases with deaging time, in contrast to the increase of the modulus during martensite aging. Although this aspect of deaging has not been found in SMAs experimentally, a similar effect has been observed in ferroelectrics, i.e. the increase of dielectric permittivity with deaging time in the paraelectric phase.[37] Thus, the effect shown in Fig. 10(a) is expected. The other phenomenon expected from our model is the time-dependence of the stress-strain response in the parent phase. From Fig. 10(b), the linear stress-strain curve becomes "flatter" with deaging time, corresponding to a decrease of the calculated

21

elastic modulus in Fig. 10(a). Experimental evidence for the above predicted phenomenon will provide further support for our model.
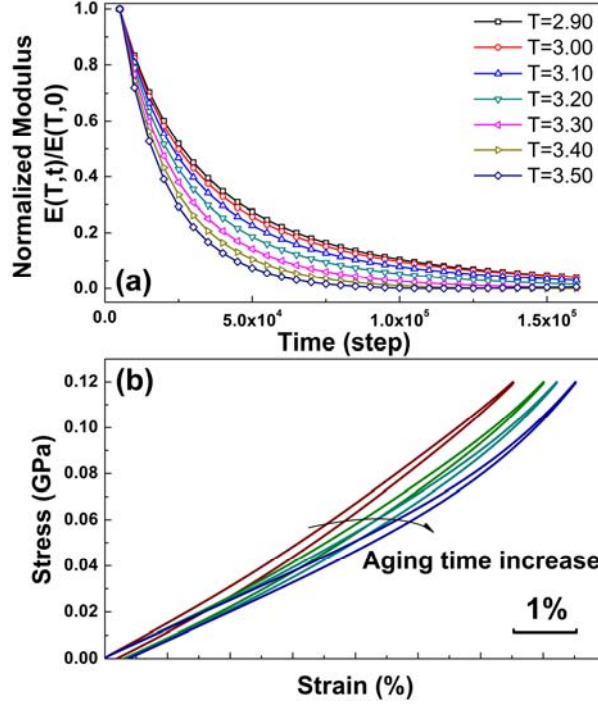

Fig.10. (a) Calculated elastic modulus and (b) stress-strain curves as a function of deaging time in the parent phase. The decrease of elastic modulus and the flattening of the stress-strain curves in the parent phase with deaging time are the predictions from our calculation. The elastic moduli are normalized by the initial values through $E(T,t)/E(T,0)$.

V.   DISCUSSION

As readily seen, martensite aging and deaging are conjugate phenomena. To be specific, martensite stabilization leads to an increase of the reverse martensitic transformation temperature whereas parent phase stabilization results in the decrease of the martensitic transformation temperature. The elastic modulus increases and decreases during the martensite aging and deaging respectively. This conjugate behavior has been achieved in our model by incorporating an increase and decrease of the same internal stress field ρ, during the martensite aging and deaging process, respectively. The internal stress field ρ is symmetry related, and the increase of ρ in the martensite will result in the decease of the free energy, as shown in Fig. 11(a1).

22

This indicates that the system evolves to a stable state where the distribution of point defects conforms to the crystal symmetry. In the parent phase, the decrease of ρ will also lead to the decrease of the free energy, as shown in Fig. 11(b1). Here the distribution of point defects will change from non-cubic to cubic symmetry, the same as the crystal lattice and give rise to a stable parent phase. Furthermore, the internal stress field ρ favors the martensite phase, so that the increase of ρ leads to an increase of the OP e_2 in the martensite and the decrease of ρ leads to a decrease of e_2 in the parent phase, as shown in Figs. 11(a2) and 11(b2). Thus, the changes in physical properties during martensite aging and deaging can be ascribed to the time dependence of the OP e_2 of the system.

As discussed previously, the martensite aging and deaging effects are generally attributed to the rearrangement of point defects within crystal lattices and the driving force is the symmetry change during martensitic transformation. Our ideas are quite general and can apply to any martensitic transformation in SMAs. The reasons why we chose FePd as an example for our modeling are 1) the square to rectangular martensitic transformation in 2D (which assumes that the system behaves in the same way in the third direction) for the FePd alloy is the simplest case that can illustrate the symmetry change during the transformation process; 2) the required parameters for the FePd alloy are available in literature. Few reports exist where the parameters are known for other SMAs. However, if the appropriate parameters for systems such as Au-Cd, Au-Cu-Zn, Cu-Zn-Al, Cu-Al-Ni, Ti-Ni-Hf and Ni-Mn-Ga, are used, then the aging and deaging behavior should be captured by our model. Our future work will be directed towards determining the parameters for other alloys. In addition, it should be mentioned that the experimental results for martensite aging effects in FePd alloys are seldom reported in the literature. This may be ascribed to the small amount of mobile point defects in FePd alloys. Finally, with the insight gleaned from our work, the aging and deaging in ferroelectric materials may be modeled. As ferroelectric materials such as $BaTiO_3$ and $PbTiO_3$ are well parameterized, the validity of our method can be further examined by comparing with the abundant experimental results available for these systems.
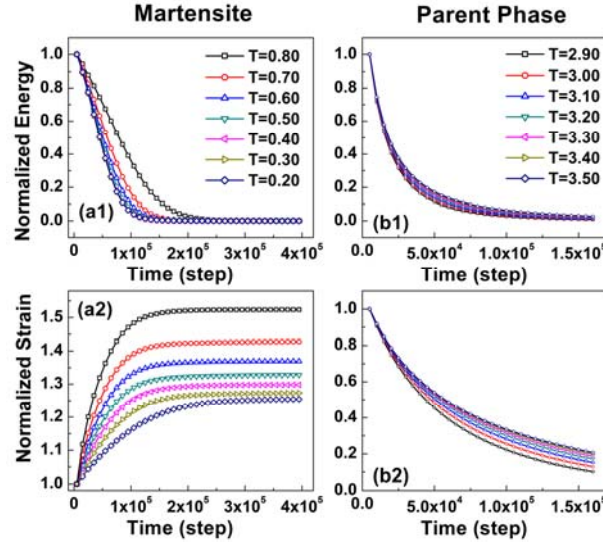
Fig.11. Evolution of free energy ((a1) and (b1)), and order parameter e_2 ((a2) and (b2)) with aging time in the martensite phase ((a1) and (a2)) and deaging time in the parent phase ((b1) and (b2)), respectively. The system evolves to a stable state (with lower free energy) in both martensite (a1) and parent phase (b1), wheras the order parameter e_2 increases in the martensite (a2) and decreases in the parent phase (b2) with time. For clearer comparison, all data are normalized by the corresponding initial values.

VI.   CONCLUSIONS

In summary, a Landau free energy model has been developed to study martensite aging and deaging effects. Time dependent Ginzburg-Landau simulations successfully reproduce experimentally observed phenomena. Based on the above simulation, the following conclusions can be made: (1) A symmetry related internal stress field can be formulated to describe the distribution change of point defects, following the SC-SRO principle. It adopts a double well profile in energy in the martensite phase and single well profile in the parent phase. (2) Martensite aging effects including martensite stabilization, rubber-like behavior, domain memory effect and aging in elastic modulus, can be ascribed to an increase of such an internal stress field. (3) Deaging effects including elimination of martensite aging and parent phase stabilization can be attributed to the decrease of the above internal stress field. (4) Elimination of martensite aging effects requires both the reverse transformation to the parent phase and sufficient deaging in the parent phase to allow adequate diffusion of point defects to occur. (5) The time dependent change of elastic modulus and the

stress-strain response in the parent phase are predictions from our model, which need to be verified experimentally.

ACKNOWLEDGEMENTS

References

[1] K. Otsuka and C. M. Wayman, *Shape Memory Materials* (Cambridge University Press, Cambridge, 1998).

[2] A. A. Arab and M. Ahlers, Acta Metall. **36**, 2627 (1988).

[3] Y. Murakami, Y. Nakajima, K. Otsuka, T. Ohba, R. Matsuo, and K. Ohshima, Mater. Sci. Eng., A **237**, 87 (1997).

[4] X. Ren and K. Otsuka, Nature **389**, 579 (1997).

[5] S. Miura, S. Maeda, and N. Nakanishi, Philos. Mag. **30**, 565 (1974).

[6] R. Santamarta, C. Seguí, J. Pons, and E. Cesari, Scripta Mater. **41**, 867 (1999).

[7] C. Seguí, E. Cesari, J. Font, J. Muntasell, and V. A. Chernenko, Scripta Mater. **53**, 315 (2005).

[8] J. Van Humbeeck, J. Janssen, N. Mwamba, and L. Delaey, Scripta Metall. **18**, 893 (1984).

[9] J. Deng, X. Ding, Z. Zhang, T. Lookman, T. Suzuki, K. Otsuka, J. Sun, A. Saxena, and X. Ren, Appl. Phys. Lett. **97**, 171902 (2010).

[10] X. Ren and K. Otsuka, Phys. Rev. Lett. **85**, 1016 (2000).

[11] K. Otsuka and X. Ren, Phase Transitions **69**, 329 (1999).

[12] K. Otsuka and X. Ren, Scripta Mater. **50**, 207 (2004).

[13] X. B. Ren and K. Otsuka, MRS Bull. **27**, 115 (2002).

[14] Y. Murakami, S. Morito, Y. Nakajima, K. Otsuka, T. Suzuki, and T. Ohba, Mater. Lett. **21**, 275 (1994).

[15] W. Cai and K. Otsuka, Scripta Mater. **41**, 1311 (1999).

[16] D. Xue, Y. Zhou, X. Ding, K. Otsuka, J. Sun, and X. Ren, Acta Mater. **59**, 4999 (2011).

[17] N. Nakanishi, T. Mori, S. Miura, Y. Murakami, and S. Kachi, Philos. Mag. **28**, 277 (1973).

[18] J. Deng, X. Ding, T. Lookman, T. Suzuki, A. Saxena, K. Otsuka, J. Sun, and X. Ren, Phys. Rev. B. **82**, 184101 (2010).

[19] J. Deng, X. Ding, T. Lookman, T. Suzuki, K. Otsuka, J. Sun, A. Saxena, and X. Ren, Phys. Rev. B. **81**, 220101 (2010).

[20] T. Ohta, Mater. Sci. Eng., A **312**, 57 (2001).

[21] T. Okuzono, Y. Yamazaki, and T. Ohta, Phys. Rev. B. **67**, 054106 (2003).

[22] V. A. L'vov, A. Kosogor, O. Soderberg, and H. Simo-Pekka, Mater. Sci. Forum **635**, 13 (2010).

[23] A. Kosogor, V. A. L'vov, O. Söderberg, and H. Simo-Pekka, Acta Mater. **59**, 3593 (2011).

[24] V. A. L'vov, A. Kosogor, J. M. Barandiaran, and V. Chernenko, Acta Mater. **60**, 1587 (2012).

[25] H. Bao, D. Xue, Y. Wang, J. Gao, L. Zhang, S. Yang, K. Yadav, and X. Ren, J. Appl. Phys. **109,** 124103 (2011).

[26] S. Kartha, J. A. Krumhansl, J. P. Sethna, and K. Wickham, Phys. Rev. B. **52**, 803 (1995).

[27] S. R. Shenoy, T. Lookman, A. Saxena, and R. Bishop, Phys. Rev. B. **60**, R12537 (1999).

[28] T. Lookman, S. R. Shenoy, K. Ø. Rasmussen, A. Saxena, and R. Bishop, Phys. Rev. B. **67**, 024114 (2003).

[29] P. Lloveras, T. Castán, M. Porta, A. Planes, and A. Saxena, Phys. Rev. Lett. **100**, 165707 (2008).

[30] G. Barceló, R. Rapacioli, and M. Ahlers, Scripta Metall. **12**, 1069 (1978).

[31] H. Sakamoto, K. Otsuka, and K. Shimizu, Scripta Metall. **11**, 607 (1977).

[32] Z. S. Basinski and J. W. Christian, Acta Metall. **2**, 101 (1954).

[33] Y. Zhou, D. Xue, X. Ding, Y. Wang, J. Zhang, Z. Zhang, D. Wang, K. Otsuka, J. Sun, and X. Ren,, Acta Mater. **58**, 5433 (2010).

[34] G. Scarsbrook and W. M. Stobbs, Acta Metall. **35**, 47 (1987).

[35] D. Z. Sun, X. B. Ren, and K. Otsuka, Appl. Phys. Lett. **87** (2005).

[36] D.Xue, J. Gao, H. Bao, Y. Zhou, L. Zhang, and X. Ren,, J. Phys.: Condens. Matter **23**, 275902 (2011).

[37] D. Xue, J. Gao, L. Zhang, H. Bao, W. Liu, C. Zhou, and X. Ren, Appl. Phys. Lett. **94**, 082902 (2009).